International Journal of Technology v(i) pp-pp (YYYY)
Received Month Year / Revised Month Year / Accepted Month Year

International Journal of Technology

http://ijtech.eng.ui.ac.id

Target Strength of Eel from Echosounder and Calibrated Fish Finder Using Acoustic Measurement and Numerical Model

Abstract. For many years, acoustics has been a critical method for surveying and assessing fish stocks in aquatic environments, using instruments such as conventional fish finder and scientific echosounder. Some fish finders contain information on acoustic backscattering, providing an opportunity to extend the application of the instrument for more scientific uses in fish exploration. On the other hand, a scientific echosounder provides more accurate measurements because of its calibrated acoustic backscattering characteristics. In this study, we investigated the acoustic backscattering of the eel (*Anguilla sp*.) using the calibrated fish finder Furuno FCV-628 and scientific echosounder Simrad EK15. Discrete fish targets were detected throughout the water column within schooling fish and as individuals by quantifying the acoustic backscattering value of the eel. Both instruments used a frequency of 200 kHz. Distorted-wave Born approximation (DWBA) dan Kirchhoff-ray mode (KRM) models were employed to estimate the theoretical dorsal and lateral backscatter as a function of frequency and length for each eel. This paper presents the results of the calibrated fish finder, demonstrating its capabilities in differentiating the acoustic response of eels compared to the results from scientific echosounders and numerical models at different lengths of fish.

Keywords: Acoustic backscattering; eel; calibrated fish finder; numerical models; scientific echosounder

1. Introduction

Eel fish, particularly in Lake Poso, Sulawesi Island, Indonesia, play a significant role in the local fishery industry due to their high potential economic and strategic position (Moeis *et al.*, 2024). The life cycle of eels encompasses various stages characterized by distinct shapes and sizes, ranging from the transparent bodies of glass eels to the more robust and pigmented forms of elvers and adult eels (Lukman *et al.*, 2021; Triyanto *et al.*, 2021). The Industrial Revolution 4.0 has brought innovative ways to monitor eels for sustainability. Technology like the underwater acoustics is now used to track eel behavior and migration patterns (Surjandari *et al.*, 2022).

The use of acoustics in fisheries research is critically important (~~Lagarde *et al.*, 2020;~~ Becker and Suthers, 2014; Lagarde *et al.*, 2020; Zang *et al.*, 2021). The industry standard for fish exploration and monitoring, especially for migratory fishes, is using a scientific echosounder to measure fish target strength (TS) (Popper *et al.*, 2020). Acoustic methods are increasingly used because they are quantitative, non-invasive, and not limited to light availability and high turbidity (Martignac *et al.*, 2015). However, they have limitations in operation, portability, and compatibility. Although attempts to measure TS using a scientific echosounder have many advantages, a calibrated fish finder can also provide acoustic backscatter information as a research tool. Both instruments can be used to rapidly calculate aquatic populations, such as fish abundance, and observe migratory movements and spatial and temporal patterns, especially for eels (*Anguilla* spp.) (MacLennan and

Fernandes, 2008; ~~Simmonds and Foote, 1997; Foote~~Howe *et al.*, ~~1987). However, compared to~~2019; Noda *et al.*, 2021; Shen *et al.*, 2024).

The fish finder's general weakness is that it does not have TS and SV outputs for post-processing. On the other hand, a scientific echosounder provides more accurate acoustic backscattering measurements. The fish data types displayed is also lack of accuracy because the fish finder is designed only for fishing. ~~, it~~It is relatively easy to calibrate the acoustic backscattering value. The signal received by the fish finder as raw uncalibrated data might contain backscatter from many objects in the water column (Winfield *et al.*, 2009). This conventional fish finder must be calibrated by measuring the echo pattern for each target, instrument setting to avoid electrical interference and false echoes to provide precise TS measurement of the targets (Demer *et al.*, 2015).

The study of eels has seen significant advancements with the application of the latest acoustic methods. These methods, as reported in recent research papers (Popper *et al.*, 2020; Noda *et al.*, 2021), have provided a more detailed understanding of their behavior and migration patterns. Among these, the use of single beam echosounders Simrad EK15 and Furuno FCV-628, both with 200 kHz frequency, has been particularly noteworthy. It is necessary to check the results obtained by the two-type acoustics instruments to give same results (Rautureau *et al.*, 2022). The Simrad EK15, with its high-resolution capabilities and compact narrowband transducer, has been instrumental in providing detailed information of acoustics characteristics of fish (Betanzos *et al.*, 2015; Linløkken *et al.*, 2019; Fauziyah *et al.*, 2023). On the other hand, the Furuno FCV-628, has provided an incredible boost in resolution (Manik *et al.*, 2020), flexible raw data output, and target separation (Dwinovantyo *et al.*, 2023), proving to be an effective tool for monitoring and studying eels in their natural habitats.

Several parameters on acoustic devices must be calibrated to achieve accurate acoustic backscatter measurement results (Demer *et al.*, 2015). Acoustic instrument calibration was

conducted by measuring sphere ball TS in the laboratory under controlled conditions (Manik *et al.*, 2017). The TS of eels was then measured with various fish lengths using these calibrated acoustic instruments. This measurement process produces variations in TS values based on different fish sizes (Pratt *et al.*, 2021; Dunning *et al.*, 2023~~; Pratt *et al.*, 2021~~). Information on the TS of each fish size was measured under controlled conditions in a small water tank with horizontal beam orientation (Kim *et al.*, 2018).

~~The~~ In the field of fish ~~finder's general weakness is that it does not have~~ measurement, comparing measured target strength (TS-) with theoretical TS derived from models such as the Kirchhoff Ray Mode (KRM) and ~~SV outputs~~Distorted Wave Born Approximation (DWBA) is essential for ~~post-processing.~~ validating experimental findings and refining~~The fish data types displayed is also lack of accuracy because the fish finder is designed only for fishing. On the other hand, a scientific echosounder provides more accurate~~ acoustic ~~backscattering measurements.~~methodologies. To measure eel's theoretical TS, the ~~Kirchhoff-ray mode (~~KRM~~)~~ model was used for elver and adult eels, ~~and distorted-wave Born approximation (~~on the other hand, DWBA~~)~~ model was used for glass eels (Horne *et al.*, 2000; Macaulay *et al.*, 2013~~; Horne *et al.*, 2000; Clay and Horne, 1994~~). This research was conducted to overcome these problems in conventional fish finders by quantifying backscatter in digital numbers, which were then converted into TS in decibels (dB). Our research fills a crucial gap in eel acoustics by combining acoustic measurements at the same frequency, offering insights that bridge empirical data with numerical models, thus advancing the understanding of eel behavior and ecology.

2. Methods

2.1. Experimental Design

~~The TS measurements of each fish were taken alternately by the fish finder and echosounder, while the TS of a sphere ball was measured as a control. The schematic setting of the interface on the fish finder and echosounder is shown in Figure 1.~~

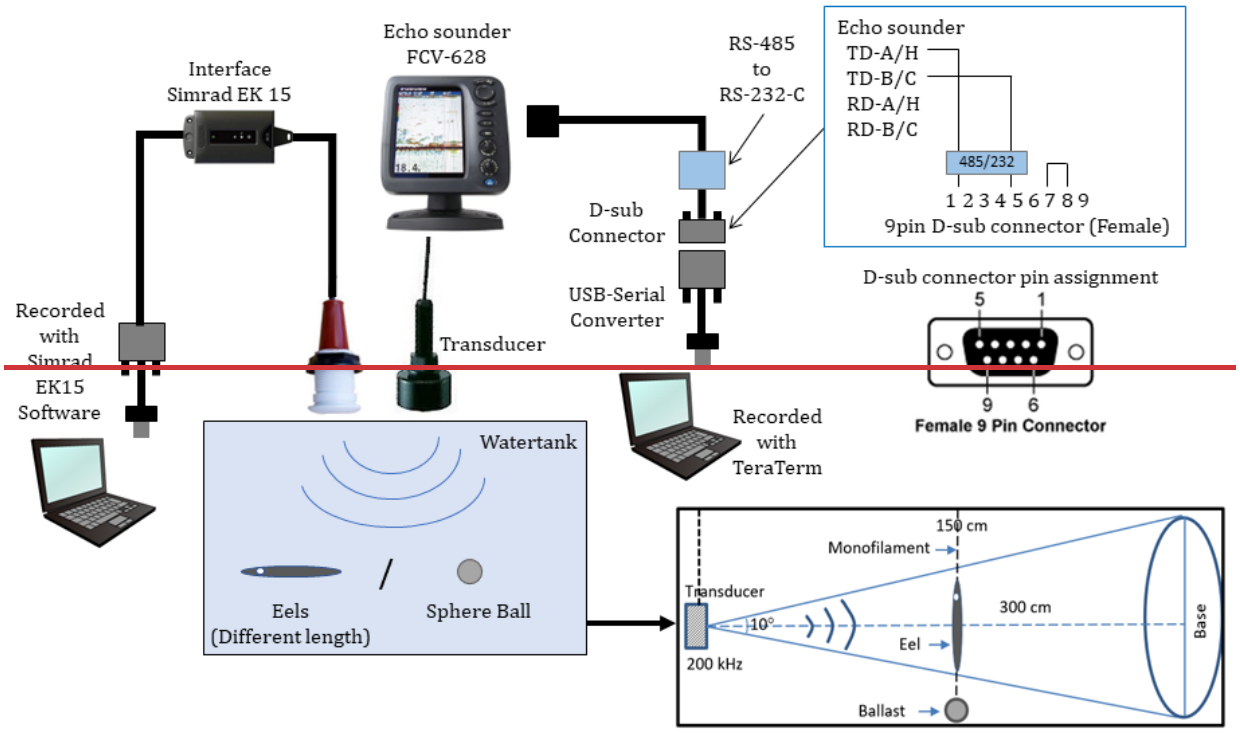

In this research experimental setup, the acoustic acquisition was conducted using alternating deployments of the scientific echosounder Simrad EK15 (Simrad Kongsberg Maritime AS, Horten, Norway) and fish finder Furuno FCV-628 (FURUNO ELECTRIC CO., LTD, Hyogo, Japan) for each individual eel across a range of lengths. Concurrently, a sphere ball was utilized to serve as a control for calibration purposes (Demer *et al.*, 2015). By systematically varying the length of the eels under investigation, the experimental design aimed to elucidate potential size-related patterns in acoustic signatures. The EK15 utilized EK15 software integrated with pre-built interface hardware, enabling direct communication and control during measurements. Conversely, the FCV-628 echo sounder was connected via a serial converter, with data acquisition and recording managed through TeraTerm software (Dwinovantyo *et al.*, 2023). The schematic setting of the interface on the fish finder and echosounder is shown in Figure 1.

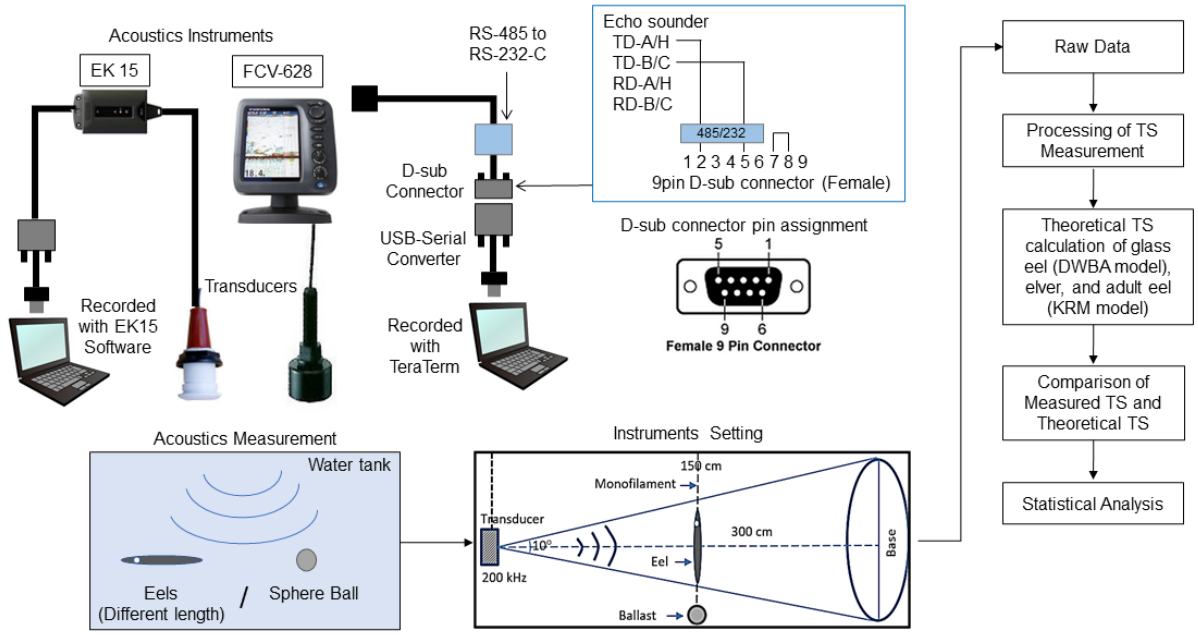

Figure 1 Schematic of experimental data acquisition for eel TS measurement in the controlled water tank contrasting acquired data with theoretical TS derived from numerical models for comprehensive analysis

Following data acquisition, the raw data from acoustic measurements were subjected to specific processing based on the sonar equation (Manik *et al.*, 2020) and comparison with KRM and DWBA model to evaluate the accuracy and consistency of the research findings. Finally, to discern any underlying relationships and trends, the statistical analysis techniques were employed specifically using simple linear regression.

2.2. Data Acquisition

The tools used were a single beam fish finder Furuno FCV-628 and single beam scientific echosounder Simrad EK15 (both with a frequency of 200 kHz), various sizes of eels, sphere ball, and monofilament line. Acoustic instrument settings are shown in Table 1.

Table 1 Tool settings during data acquisition and water conditions in the water tank

Parameter	Furuno FCV-628	Simrad EK-15
Beam type	Single beam	Single beam

Absorption coef. (dB m^{-1})	0.007195	0.007195
The frequency used (kHz)	200	200
Power (W)	600	1000
Transmission rate (ms)	0.1	1.02
Beam width (°)	10	26
Sound speed (ms^{-1})	1501	1501
Data format	*.csv	*.raw
Temperature (°C)	27	27
Salinity (psu)	0	0

The research procedure consisted of calibrating the fish finder using a sphere ball and then measuring the acoustic data of eels by each instrument in the water tank with a water temperature of 27 °C. TS measurements were taken on 69 live eels with sizes varying from 6.5 to 90 cm. The eels were anesthetized as they were still alive when their TS was measured. The transducers were mounted horizontally about 0.5 m below the water with various eel orientation (Kurnia *et al.*, 2011; Kerschbaumer *et al.*, 2020~~; Kurnia *et al.*, 2011~~).

2.3. Data Analysis

Data processing in this research included acoustic data processing to convert raw data into acoustic backscattering values in decibels (dB). The raw data were obtained from the TeraTerm software for the fish finder Furuno FCV-628 and Simrad EK15 Acquisition version 1.2.4 software for the scientific echosounder. When an acoustic signal hits the targets or objects, the characteristic measure of the scattering strength is considered to be the specific scattering power (Nishiyama, 2017) as Equation 1.

$$TS = EL - KTR + 40logR + 2\alpha R - 120 \quad (1)$$

where *TS* is target strength (dB), *EL* is echo level (dBμV), *KTR* is the factor of transmitting and receiving (dBV), *R* is water range from the transducer to object (m), and α is ~~Absorption~~absorption coefficients (dB km^{-1}). The KTR is an unknown parameter for users and was calibrated by the manufacturer. The measured TS from both instruments were then compared (Rautureau *et al.*, 2022)

The observed fish TS was considered a function mainly of the fish's length and orientation or angle of inclination. The length of the fish and the angle of inclination of the observed fish are shown in Equation 2 (Sawada ~~and~~ *et al.*, 1993; Furusawa~~, 1993~~ and Amakasu, 2010):

$$\begin{aligned} T_{S(0)} &= \int\int f_a(\theta) f_b(L) T_S(\theta, L)\, \mathrm{d}\theta \mathrm{dL} \\ &= \int f_b(L)\mathrm{dL} \int f_a(\theta) T_S(\theta, L)\, \mathrm{d}\theta \end{aligned} \quad (2)$$

where *L* is the length of the fish (m), θ is the angle of inclination of the fish (°), $f_a(\theta)$ is the probability density function (PDF) of the tilt angle, and $f_b(L)$ is the PDF of the length of the fish. The results of measuring the reflected acoustic strength with variations in the angle and acoustic sounding points on each target's back (dorsal), abdomen (ventral), and side were compared and averaged to obtain the average TS value. The Equation 2 can be derived from the relationship between the length and the average TS in Equation 3 as follows:

$$\begin{aligned} T_{S(0)} &= T_{S(\mathrm{cm})} \int L^2 f_b(L)\mathrm{dL} \\ &= T_{s(\mathrm{cm})} \left[\left\{ \int L f_b(L)\mathrm{dL} \right\}^2 + {\sigma_L}^2 \right] \\ &= T_{s(\mathrm{cm})} \left({L_{Avg}}^2 + {\sigma_L}^2 \right) \end{aligned} \quad (3)$$

where L_{Avg} is the mean of fish length, and ~~L~~σ_L is the standard deviation. The following calculation is TS_{cm} from the average TS measured and the average fish length, along with the standard deviation obtained from the measured fish length (Dunning *et al.,* 2023). Assuming that the standard deviation of the variation in fish length is relatively small. The averaged TS is assumed to be equal to the mean TS of the fish.

2.4. Numerical Model

In this study, two numerical models were used, which have different uses for each form of eel. The KRM model was used for theoretical TS calculations on adult eels, while the DWBA model was used for TS calculations of glass eels and elver or eel in the juvenile phase.

2.4.1. Kirchhoff-ray Mode (KRM) Model

A KRM model was used to theoretically estimate acoustical backscattering characteristics of eels' dorsal and lateral as a function of fish length, aspect, and frequency (~~Clay and Horne, 1994).~~Lan-yue *et al.,* 2021). This model uses a fish shape base resembling fluid and gas-filled cylinders representing the body and swimbladder, respectively. The acoustic backscattering for the fish body is expressed in Equation 4 as:

$$l(\mathrm{f}) = -\mathrm{i}\frac{R_{fs}(1-R_{wf}^2)}{2\sqrt{\pi}}\sum_{j=0}^{N-1} A_{sb}[k_{fb}a(j)+1]^{\frac{1}{2}}\left[e^{-i(2k_{fb}V_{U(j)}+\psi_{sb})}\right]\Delta u(j) \quad (4)$$

and swimbladder expressed in Equation 5 as:

$$l(\mathrm{f}) = -\mathrm{i}\frac{R_{wf}}{2\sqrt{\pi}}\sum_{j=0}^{N-1}[k\,a(j)]^{\frac{1}{2}}\left[e^{-i2kV_j} - \left(1-R_{wf}^2\right)e^{i(-2kv_{u(j)}+2k_{fb}(V_U(j)-V_L(j)+\psi_{fb})}\right]\Delta u(j) \quad (5)$$

where $l(\mathrm{f})$ is scattering amplitude as a function of carrier frequency, k is the wave number ($2\pi/\lambda$) which depends on the frequency and sound speed at water medium, λ is the acoustical wavelength, a is the radius of the cylinder, *fb* is the fish body, *w* is water, *sb* is swimbladder, and $\Delta u(j)$ is the cumulative distance between cylinder at the midpoint (Li *et al.,* 2023). The backscattering cross-section (σ_{bs}) from the scattering amplitude was calculated in Equation 6, so the theoretical TS of the eels can be written in Equation 7 as:

$$\sigma_{bs} = \frac{|l(\mathrm{f})|^2}{TL^2} \quad (6)$$

$$TS = 20\log_{10}\left[\frac{l(\mathrm{f})}{TL}\right] \quad (7)$$

where TL is transmission losses, the theoretical TS was calculated individually for the fish body and swimbladder, then summed to get the whole fish to scatter for theoretical TS.

2.4.2. Distorted-wave Born Approximation Model for Glass Eel and Elver

General mathematical equations for scattering amplitude in DWBA model can be written in Equation 8 as follows:

$$f_{bs} = \frac{k_1^2}{4\pi}\iiint_V (\gamma_\kappa - \gamma_\rho)\exp i2(\vec{k}_i)_2 \cdot \vec{r}_{pos}\ \mathrm{dv} \quad (8)$$

where f_{bs} is the backscattering amplitude, k_1 is the acoustic wave number, r_0 is the position vector, $\vec{r}_{pos}$ value is the position in a particular line of the body axis. The material properties of glass eel and elver bodies, γ_ρ, and γ_κ were expressed in Equation 9 as (Jech *et al.,* 2015):

$$\gamma_\rho \equiv \frac{\rho_2-\rho_1}{\rho_2} = \frac{g-1}{g}$$
$$\gamma_\kappa \equiv \frac{\kappa_2-\kappa_1}{\kappa_2} = \frac{1-gh^2}{gh^2} \quad (9)$$

where g is density contrast, h is sound speed contrast, and κ is compressibility and can be written in Equation 10 as:

$$\kappa = (\rho c^2)^{-1} \quad (10)$$

where ρ is mass density, and c is sound speed. The DWBA model is used in weak scatterers and is valid for all acoustic frequencies, the angle of orientation, and shapes of glass eel and elver. We considered using g and h from other research based on the acoustic properties of the weakly scattering sphere of fluid-like bodies (~~Medwin, 2005~~Jech *et al.*, 2015). Density (ρ) and sound speed (c) in the glass eel and elver bodies were 1028 kg m^{-3} and 1480.3 m s^{-1}, respectively, against the surrounding medium of 1026.9 kg m^{-3} and 1477.4 m s^{-1} (Kusdinar *et al.*, 2014).

3. Results and Discussion

3.1. Calibration

The results of the fish finder calibration using a sphere have produced output data in the form of raw data, which were then extracted using spreadsheet software. The output data consists of index of setting, depth, and echo data record as shown in Figure 2.

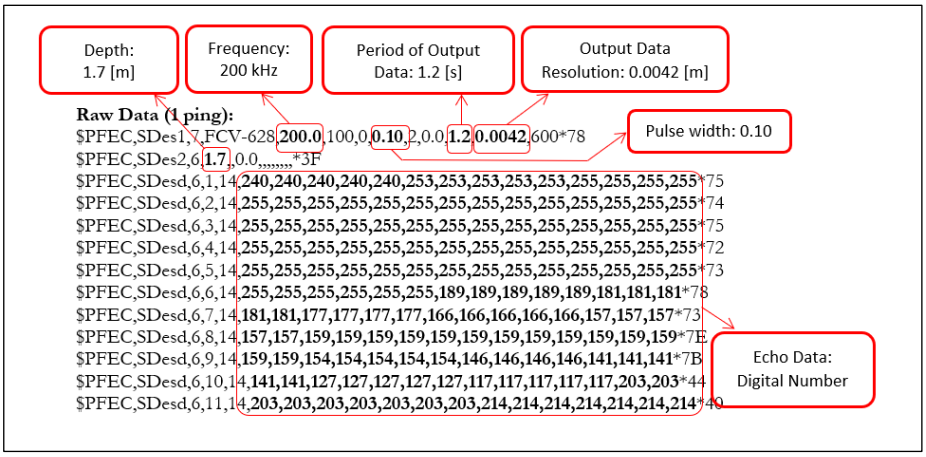

Figure 2 Raw data output in one ping data from the fish finder

The data format was NMEA0183 proprietary sentence compatible with a baud rate of 38400bps. In the raw data, PFEC SDes1, which contained frequency, power, pulse width, data type, start depth, resolution, and the number of data, was used to index the setting. PFEC SDes2 contained the depth of measurement, while PFEC SDesd contained raw echo data from an echo sounder without TVG compensation.

The calibration was conducted to verify whether this fish finder could measure the sphere ball (Kim *et al.*, 2018). The TS pattern was calculated and compared to the theoretical model, and the measured TS results agreed with the model, confirming its accuracy. Data from recorded pings were compared and averaged to verify data consistency. The calibration results are shown in Figure 3.

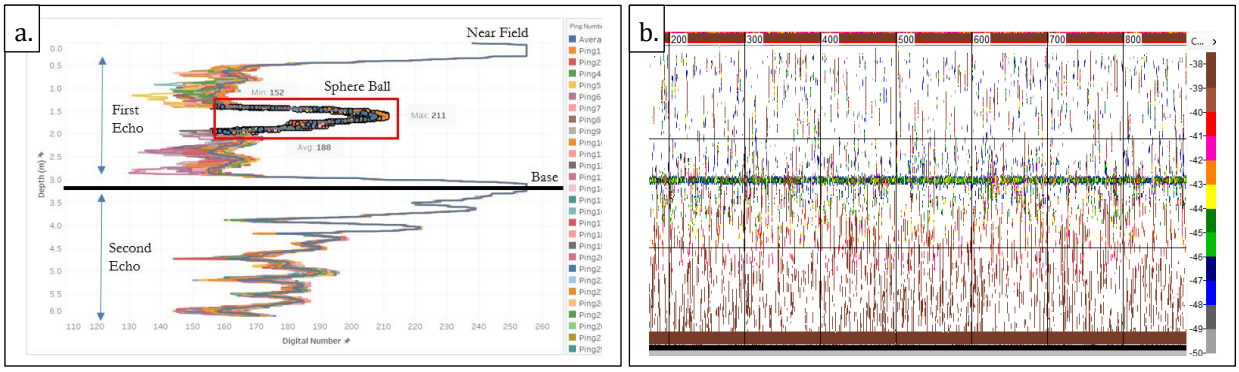

Figure 3 (a) The raw data and (b) processed data of the sphere ball from the fish finder

Figure 3 (a) represents the presence of a first echo and a second echo on each ping from the TS measurements. The first echo showed backscattering from the water's surface to the bottom which also shown the sphere ball backscattering strength, while the second echo showed the reflection back by the bottom of the water. The measurement results also showed noise on the surface caused by the near field at 0-0.5 m.

The results obtained were an average value of 188 from 100 pings, a minimum value of 152, and a maximum of 211. The reflected strengths were then processed into decibels (dB). Figure 3 (b) represents the sonar equation conversion results as echogram which considered many parameters, such as transmission losses and sound absorption by the water medium. The average TS of the sphere using Equation 1 was -40.55 dB, with the theoretical TS for a standard sphere ball being -41.0 dB (Demer *et al.*, 2015).

3.2. Measured TS pattern and orientation of eels

The average echo isolation was used which generally isolates the measured echo value from the received reflection (Dunning *et al.*, 2023). If the average peak echo value criteria are significantly higher than the surrounding echo value, the echo is considered a single echo. The TS values obtained from the variation of the measurement angle was on the dorsal, ventral, and both sides of the eel, shown in Figure 4.

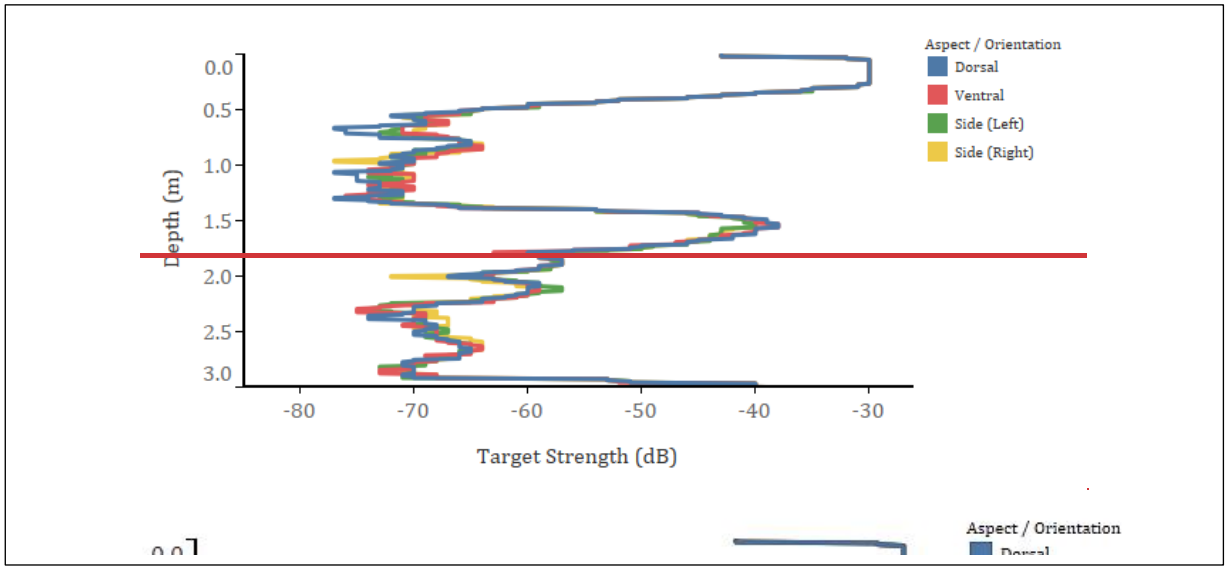

Figure 4 The results of measuring acoustic values on the dorsal or upper side (blue), ventral or down side (red), left side (green), and right side (yellow) of the eel

Eels were measured at a 1.4-1.6 m depth, with a higher acoustic peak. The value on the dorsal side can be higher because the entire surface of the head and the swim bladder were reflected back the sound, so the digital value obtained is high. These swimbladder are filled with air, making their acoustic value higher due to the difference in acoustic impedance between water and air (Gauthier and Horne, 2004).

3.3. TS of eels from Numerical Models

3.3.1. KRM Model

The comparison between the measured target strength of fish in a laboratory and target strength from the KRM model can vary depending on factors such as the type of fish, the experimental setup, and the modeling assumptions made in the Kirchhoff ray mode model (Reeder *et al.*, 2004). The result was based on certain assumptions about the fish's shape, size, and composition (Kusdinar *et al.*, 2014). Based on our experiments, the KRM model was used only for adult eels because it could model TS from all frequencies and

measured near-normal incidence. Combining experimental measurements and modeling approaches can provide a more comprehensive understanding of fish target strength and variability, shown in Figure 5.

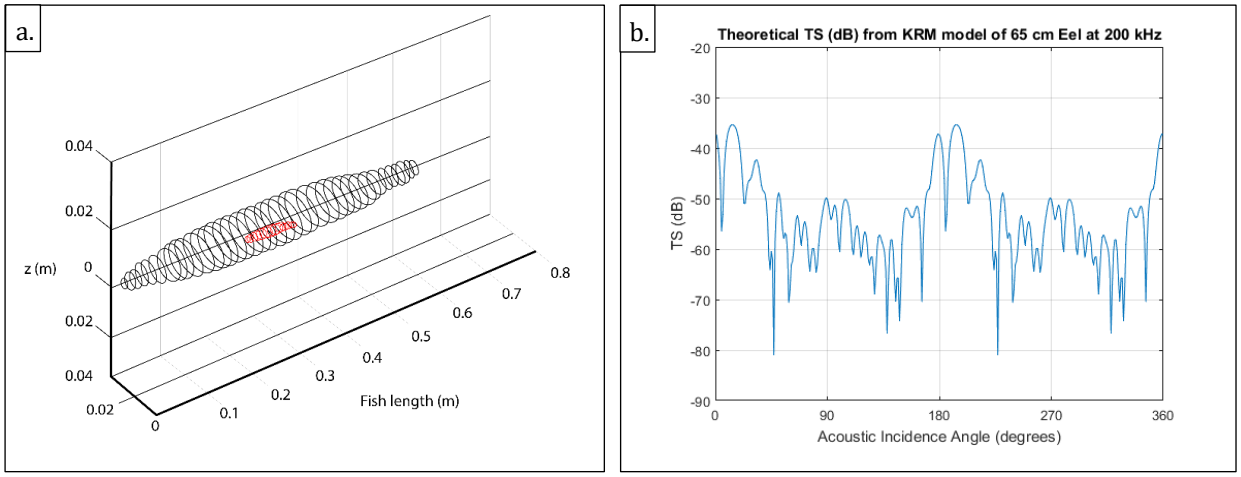

Figure 5 (a) Digitized shape of eels in cylinder form with swim bladder (red color) with interval 16 mm; (b) The theoretical TS pattern related to tilting angle from digitized shape of eel generated by KRM model

The TS values generated from the KRM model showed various results based on the acoustic incidence angle or fish orientation. The KRM model calculates the acoustic backscatter from a three-dimensional representation of a fish swimbladder and body (Macaulay *et al.*, 2013). The acoustic scattering pattern at 200 kHz digitizing interval of the fish and swim bladder form shown at Figure 5 (a). The modelled TS pattern in Figure 5 (b) was from integration between the fish body and swimbladder. The results in Figure 5 (b) can vary with pitch angle shifts, with the impact on fish scattering strength being greater at higher frequency. The TS values are greatest at a pitch angle range of -10° to 0°, which is related to the angle of the swimbladder tilt (Tong *et al.*, 2022).

The orientation of the fish concerning the incident sound wave can affect the TS values, as fish may exhibit different scattering characteristics in different directions. The main lobe at 0° (dorsal aspect) and 180° (ventral aspect) of incidence angle from 65 cm of eels at 200 kHz has almost the same shape with a higher TS value. A fish's dorsal and ventral aspect may have a higher scattering angle than other aspects, resulting in stronger scattering of the sound waves and higher TS values (Reeder *et al.*, 2004). All eel size was modelled, and was found the same result. The acoustics response from different size of eels primarily depends on the area and rugosity of the swim-bladder surface and their body. Fish with swim bladders may exhibit resonance effects at particular acoustics responses, leading to enhanced or reduced TS values depending on the incident frequency and swim bladder characteristics such as size, shape, and gas content (Li *et al.*, 2023).

3.3.2. DWBA Model

KRM model may have limitations when it comes to weak scatterers, such as small fish or fish in early life stages like glass eels and elvers (Jech *et al.*, 2015). This is because the KRM model is based on ray theory, which assumes that the scatterers are much larger than the wavelength of the incident sound wave and that the scattered waves are primarily due to specular reflection from the surface of the scatterer (Li *et al.*, 2023).

Glass eels and elvers are small and have relatively smooth bodies, which may not meet the assumptions of the KRM model. In such cases, a more suitable model for scattering

prediction is the distorted-wave Born approximation (DWBA) model, a more advanced scattering model that can handle smaller and weaker scatterers (Jech *et al.*, 2015). The DWBA model considers the size and shape of the scatterers, as well as their composition and orientation, and provides more accurate predictions for scattering from weak scatterers like glass eels and elvers. The fish shape was digitized for mesh generation to obtain TS from the DWBA model shown in Figure 6.

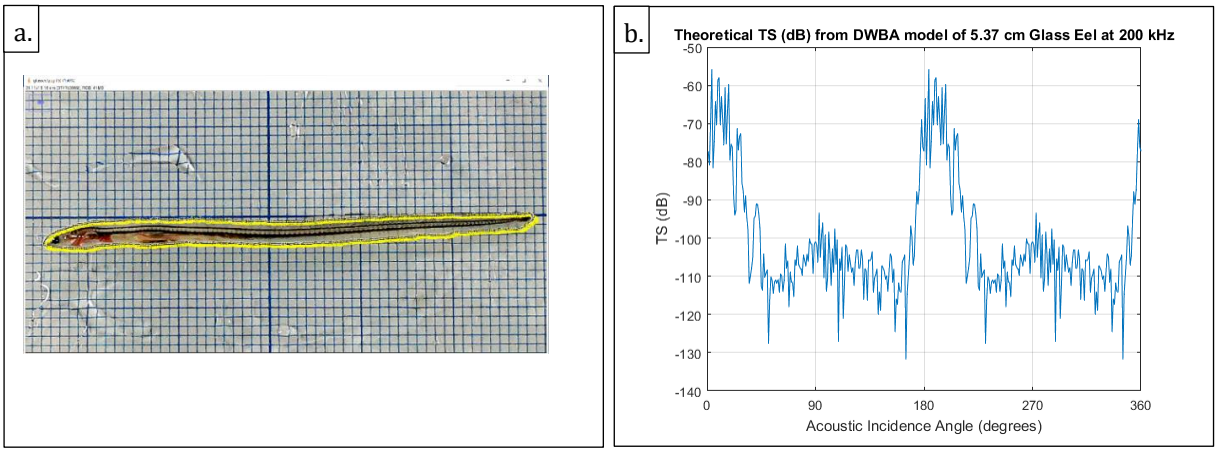

Figure 6 (a) The digitized 5.37 cm glass eel; (b) The theoretical TS compared to the acoustic incidence angle at 200 kHz generated by DWBA model

The dorsal and ventral aspects of a fish which is 0° and 180° of incidence angle, respectively, are typically more exposed to the incident sound wave as it faces toward the sound source. This can result in a more direct scattering of the sound waves from the dorsal and ventral aspects, leading to higher TS values. Additionally, a fish's body shape and orientation may affect how it scatters sound waves. The dorsal and ventral aspect has a larger surface area and may scatter more sound energy, resulting in higher TS values.

The TS curves obtained through the application of the KRM model consistently exhibited smoother frequency response profiles and lesser amplitude fluctuations. This suggests that the TS estimations derived from the KRM model demonstrate reduced variability and possess greater statistical robustness across the frequency spectrum when compared to those generated by the DWBA model. As per the central limit theorem, as the sample size expands, both the range and standard deviation are expected to diminish, as depicted in Figure 5 (b) and Figure 6 (b).

3.4. Statistical analysis

After obtaining the TS values of the eel from both numerical models, the data were plotted to determine the TS values based on their size. The numerical models were compared with the laboratory measurement results, which can be seen in Figure 7.

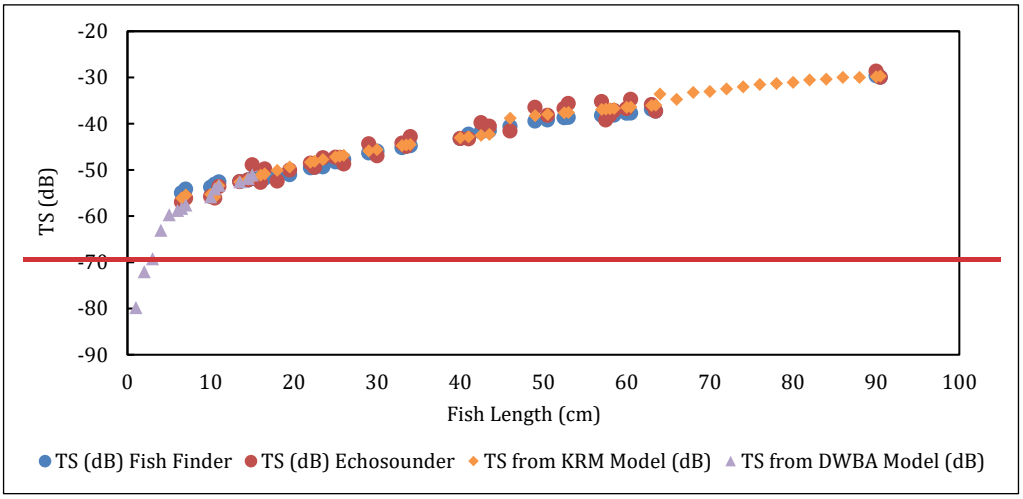

Figure 7 TS results (dB) from the direct measurements in the laboratory and the two numerical models, compared to the length of the eel (in cm)

The purple color shown in Figure 7 indicates the TS value from the DWBA model results based on the length of the eel which was taken from digitized images of the eel during the glass eel phase. The orange color indicates the TS value from the KRM model results, starting from the elver phase to adult eel. The results from both models need to be further analyzed using simple linear regression analysis. The TS values obtained from the KRM model show a good correlation with the measured TS values, as indicated by the parallel linear line, while the TS values obtained from the DWBA model tend to be higher, shown in Figure 8.

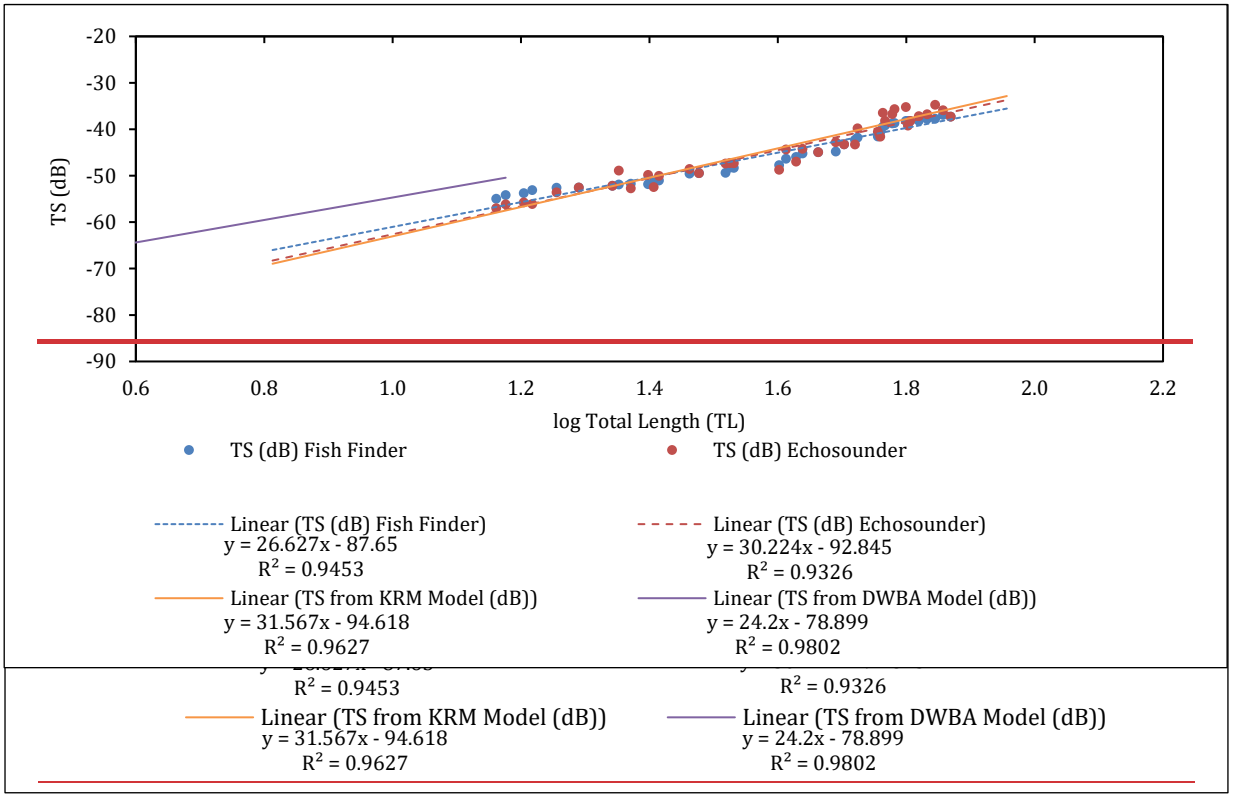

Figure 8 The results of numerical models and laboratory measurements using simple linear regression analysis

The KRM model is more suitable for solid-shaped fish, while the DWBA model is more suitable for soft-bodied organisms such as zooplankton (Jech *et al.*, 2015). The DWBA model assumes that the target organism is soft and has a smooth surface, which is not the case for elver and adult eel that have complex shapes and ~~rugh~~rough surfaces with swimbladder inside the body. The DWBA model may not be able to accurately account for the scattering and reflection of sound waves from the rough surface of the fish, leading to an overestimation of the TS value. In this study, it was not possible to differentiate between the measurements obtained in the laboratory and the DWBA model for fish with a length of 1 to 5 cm.

TS values from both results from modelling and measurement were positively related to fish length (Hananya *et al.* 2020; Dunning *et al.*, 2023~~; Hananya *et al.* 2020~~). Previous studies have linked fish length to TS on different fish species in marine ecosystem (Frouzova *et al.*, 2005). This latter study found high correlation between TS from echosounder and fish finder compared to the KRM and DWBA model. We acknowledge several limitations of the present study. This research was conducted in two eels species; *Anguillla bicolor bicolor* and *Anguilla marmorata.* Eels exhibit diverse characteristics and behaviours across different species, and their length-TS relationships could vary significantly.

The TS measurements obtained from the echosounder and calibrated fish finder were also compared, revealing no significant difference in the mean TS across different lengths of eels, as determined by a simple linear regression test (p-value > 0.05). Additionally, graphical representations of the TS values in Figure 8 demonstrate similarities between the datasets collected by the EK15 and FCV-628 echosounders, irrespective of the eels' size.

The significant impact and advantages of this study lie in its potential applications and cost-effectiveness. The study demonstrates that a calibrated fish finder can be used to accurately measure the different size of fish in a water column. To enhance the validity and generalizability of the analysis, future studies could consider expanding the sample size to

include a wider range of eel species. Additionally, examining eels from various geographic locations or ecological contexts would further enhance the applicability and robustness of the findings. For future research, data collected from the acoustics instruments can be analyzed using artificial intelligence (AI), with machine learning algorithms identifying patterns and trends (Berawi, 2020), especially for the eels' monitoring. AI can be used to automate routine and repetitive tasks in acoustics data acquisition and processing (Asvial *et al*., 2023).

4. Conclusions

The TS measurement method was applied to 69 eels in a small water tank using a calibrated fish finder at 200 kHz. There was a close relationship between eel body length and target strength. The acoustic study results showed that eels with longer body lengths had a more significant TS value. The peak of the TS value was on the dorsal and ventral aspects, while the TS value from the side aspect was lower than other aspects. Both fish finder and echosounder can provide accurate measurements of TS under controlled conditions. The simulation results of the KRM model showed a positive correlation with the laboratory measurements of TS. In contrast, the simulation results of the DWBA model tended to produce higher values of TS. The positive correlation between the KRM simulation results and the laboratory measurements suggests that the KRM model may be a more accurate tool for predicting TS values in fish. A calibrated fish finder can provide new insight for eel detection and observation of their size based on the TS value.

Acknowledgments

The authors thank the Ministry of Finance of the Republic of Indonesia for funding this research activity through the LPDP RISPRO INVITASI program 2020. All authors declare that they have no competing interests related to this manuscript.

References

Asvial, M., Zagloel, T.Y.M., Fitri, I.R., Kusrini, E., Whulanza, Y., 2023. Resolving engineering, industrial and healthcare challenges through AI-driven applications. *International Journal of Technology*, Volume 14(6), pp. 1177-1184

Becker, A., Suthers, I.M., 2014. Predator driven diel variation in abundance and behaviour of fish in deep and shallow habitats of an estuary. *Estuarine, Coastal and Shelf Science,* Volume 144, pp. 82–88

~~Clay, C.S., Horne, J.K., 1994. Acoustic model of fish: the Atlantic cod (*Gadus morhua*). *The*~~Berawi, M.A., 2020. Managing artificial intelligence technology for added value. *International Journal of ~~the Acoustical Society of America~~Technology*, Volume ~~96(3~~11(1), pp. ~~1661-1668~~1-4

Betanzos, A., Martín, H. A., Tizol, S. V. R., Schneider, P., Hernández, J. L., Brehmer, P., Linares, E. O., Guillard, J., Hermand, J.-P., 2015. Performance of a low cost single beam echosounder: In situ trials in a shallow water coral reef habitat with verification by video. *2015 IEEE/OES Acoustics in Underwater Geosciences Symposium (RIO Acoustics)*, pp. 1–3

Demer, D. A., Berger, L., Bernasconi M., Bethke, E., Boswell, K. M., Chu, D., Domokos, R., Dunford, A., Fässler S., Gauthier S., 2015. Calibration of acoustic instruments. *ICES Cooperative Research Report,* Volume 326, pp. 1-133

Dunning, J., Jansen, T., Fenwick, A., Fernandes, P., 2023. A new in-situ method to estimate fish target strength reveals high variability in broadband measurements. *Fisheries Research,* Volume 261, p. 106611

~~Foote, K.G., Knudsen, F.R., Vestnes, G., MacLennan, D.N., Simmonds, E.J., 1987. Calibration of acoustic instruments for fish density estimation: a practical guide. *ICES Cooperative Research Report,* Volume 144, pp. 1-69~~

Dwinovantyo, A., Solikin, S., Triwisesa, E., Triyanto, T., Target strength of Nile tilapia (*Oreochromis niloticus*) from 200 kHz calibrated fish finder and scientific echosounder: laboratory measurement and modelling. *IOP Conference Series: Earth and Environmental Science*, Volume 1251, p. 012022

Fauziyah, F., Ningsih, E.N., Arnando, E., Fatimah, F., Agustriadi, F., Supriyadi, F., 2023. Effect of hauling and soaking time of stationary lift nets on fish aggregation using a hydroacoustic monitoring approach. *The Egyptian Journal of Aquatic Research*, Volume 49(3), pp. 339-346

Frouzova, J., Kubecka, J., Balk, H., Frouz, J., 2005. Target strength of some European fish species and its dependence fish body parameters. *Fisheries Research,* Volume 75, pp. 86-96

Furusawa, M., Amakasu, K., 2010. The analysis of echotrace obtained by a split-beam echosounder to observe the tilt-angle dependence of fish target strength in situ. *ICES Journal of Marine Science*, Volume 67, pp. 215–230

Gauthier, S., Horne, J.K., 2004. Potential acoustic discrimination within boreal fish assemblages. *ICES Journal of Marine Science*, Volume 61(5), 836–845

Hananya, A., Pujiyati, S., Hasbi, M.S., Retnoaji, B., 2020. Indonesian short fin eel Anguilla bicolor (Mclelland, 1844) swim bladder as important organ for reflecting acoustic wave. *IOP Conf. Series: Earth and Environmental Science* 429, p. 012017

Horne, J. K., Walline, P. D., Jech, J.M., 2000. Comparing acoustic model predictions to in situ backscatter measurements of fish with dual-chambered swimbladders. *Journal of fish Biology,* Volume 57(5), pp. 1105-1121

Howe, B.M., Miksis-Olds, J., Rehm, E., Sagen, H., Worcester, P.F., Haralabus, G., 2019. Observing the oceans acoustically. *Frontiers in Marine Science,* Volume 6, p. 426

Jech, J.M., Horne, J.K., Chu, D., Demer, D.A., Francis, D.T., Gorska, N., Jones, B., Lavery, A.C., Stanton, T.K., Macaulay, G.J., Reeder B., Sawada, K., 2015. Comparisons among ten models of acoustic backscattering used in aquatic ecosystem research. *The Journal of the Acoustical Society of America,* Volume 138, pp. 3742–3764

Kerschbaumer, P., Tritthart, M., Keckeis, H., 2020. Abundance, distribution, and habitat use of fishes in a large river (Danube, Austria): mobile, horizontal hydroacoustic surveys vs. a standard fishing method. *ICES Journal of Marine Science,* Volume 77 (5), pp. 1966-1978

Kim, H., Kang, D., Cho, S., Kim, M., Park, J., Kim, K., 2018. Acoustic Target Strength Measurements for Biomass Estimation of Aquaculture Fish, Redlip Mullet (*Chelon haematocheilus*). *Applied Science,* Volume 8, ~~ppp~~. 1536

Kurnia, M., Iida, K. Mukai, T., 2011. Measurement and modelling of three-dimensional target strength of fish for horizontal scanning sonar. *Journal of Marine Science and Technology,* Volume 19(3), pp. 287-293

Kusdinar, A., Hwang, B.-K., Shin, H.-O., 2014. Determining the target strength bambood wrasse (*Pseudolabrus japonicus*) using Kirchhoff-ray mode. *Journal of the Korean society of Fisheries Technology,* Volume 50(4), pp. 427–434

Lagarde, R., Peyre, J., Amilhat, E., Mercader M., Prellwitz, F., Simon, G., Faliex, E., 2020. In situ evaluation of European eel counts and length estimates accuracy from an acoustic camera (ARIS). *Knowledge and Management of Aquatic Ecosystems,* Volume 421, p. 44

Lan-yue, Z., Yu-tong, S., Yi, Y., De-sen, Y., Gui-lin, Z., 2021. Study on acoustic scattering characteristics of fish. In *2021 OES China Ocean Acoustics (COA)*, pp. 250-255

Li, C., Chu, D., Horne, J., Li, H., 2023. Comparison of ~~Coherent~~coherent to ~~Incoherent~~incoherent Kirchhoff-~~Ray-Mode~~ray-mode (KRM) ~~Models~~models in ~~Predicting Backscatter~~predicting backscatter by ~~Swim-Bladder-Bearing Fish.~~swim-bladder-bearing fish. *Journal of Marine Science and Engineering,* Volume 11(3), p. 473

Linløkken, A.N., Næstad, F., Langdal, K., Østbye, K., 2019. Comparing fish density and echo strength distribution recorded by two generations of single beam echo sounders. *Applied Sciences*, Volume 9(10), p. 2041.

Lukman, L., Triyanto, T., Haryani, G.S., Samir, O., Gogali, L., Bandjolu, K.P., 2021. Eel (*Anguilla* spp.) fishing activity in Poso Area Central Sulawesi, Indonesia. *IOP Conference Series: Earth and Environmental Science*, Volume 869, p. 012022

Macaulay, G. J., Peña, H., Fässler, S. M., Pedersen, G., Ona, E., 2013. Accuracy of the Kirchhoff-approximation and Kirchhoff-ray-mode fish swimbladder acoustic scattering models. *PloS one,* Volume 8(5), p. e64055

MacLennan, D.N., Fernandes, P.G., 2008. Fish abundance estimation using hydroacoustics. In: Simmonds, J. (Ed.), *Fisheries Acoustics: Theory and Practice*. Blackwell Publishing Ltd, Oxford, UK, pp. 145-200

Manik, H.-M., Apdillah, D., Dwinovantyo, A., Solikin, S., 2017. Development of Quantitative Single Beam Echosounder for Measuring Fish Backscattering. *InTech*, pp. 119-133

Manik, H.M., Nishimori, Y., Nishiyama, Y., Hazama, T., Kasai, A., Firdaus, R., Elson, L., Yaodi, A., 2020. Developing signal processing of echo sounder for measuring acoustic backscatter. *IOP Conference Series: Earth and Environmental Science*, Volume 429, p. 012034

Martignac, F., Daroux, A., Bagliniere, J-L., Ombredane, D., Guillard J., 2015. The use of acoustic cameras in shallow waters: new hydroacoustic tools for monitoring migratory fish population. A review of DIDSON technology. *Fish and Fisheries,* Volume 16(3), pp. 486–510

~~McCarthy, T.K., Frankiewicz, P., Cullen, P. Blaszkowski, M., O'Connor, W., Doherty, D., 2008. Long-term effects of hydropower installations and associated river regulation on River Shannon eel populations: mitigation and management. *Hydrobiologia,* Volume 609, pp. 109–124~~

Moeis, A.O., Gita, A.A., Destyanto, A.R., Rahman, I., Hidayatno, A., Zagloel, T.Y., 2024. Policy analysis of coastal-based special economic zone development using system dynamics. *International Journal of Technology*, Volume 15(1), pp. 195-206

Noda, T., Wada, T., Mitamura, H., Kume, M., Komaki, T., Fujita, T., Sato, T., Narita, K., Yamada, M., Matsumoto, A., Hori, T., Takagi, J., Kutzer, A., Arai, N., Yamashita, Y., 2021. Migration, residency and habitat utilisation by wild and cultured Japanese eels (*Anguilla japonica*) in a shallow brackish lagoon and inflowing rivers using acoustic telemetry. *Journal of Fish Biology*, Volume 98(2), pp. 507–525

Nishiyama, Y. 2017. Easy measurement system by using conventional echo sounder. In: *The Asian Fisheries Acoustic Society (AFAS)*, Guangzhou, China

Popper, A.N., Hawkins, A.D., Jacobs, F., Jacobson, P.T., Johnson, P., Krebs, J., 2020. Use of sound to guide the movement of eels and other fishes within rivers: a critical review. *Reviews in Fish Biology and Fisheries,* Volume 30, pp. 605–622

Pratt, T.C., Stanley, D.R., Schlueter S., La Rose, J.K.L., Weinstock, A., Jacobson, P.T., 2021. Towards a downstream passage solution for out-migrating American eel (*Anguilla rostrata*) on the St. Lawrence River. *Aquaculture and Fisheries,* Volume 6-(2), pp. 151-168

Rautureau, C., Goulon, C., Guillard, J., 2022. In situ TS detections using two generations of echo-sounder, EK60 and EK80: the continuity of fishery acoustic data in lakes. *Fisheries Research*, Volume 248, p. 106237

Reeder, D.B., Jech, J.M., Stanton, T.K., 2004. Broadband acoustic backscatter and high-resolution morphology of fish: Measurement and modeling. *The Journal of the Acoustical Society of America*, Volume 116, pp. 747-761

Sawada, K., Furusawa, M., Williamson, N.J., 1993. Conditions for the precise measurement of fish target strength in situ. *The Journal of the Marine Acoustics Society of Japan,* Volume 20-(2), pp. 73-79

~~Simmonds,~~Shen, W., Peng, Z., Zhang J., ~~Foote, K.G., 1997. Acoustic scattering from zooplankton~~2024. Identification and ~~micronekton in relation to knowledge~~counting of ~~marine populations. *ICES*~~fish targets using adaptive resolution imaging sonar. *Journal of Fish Biology*, Volume 104(2), pp. 422-432

Surjandari, I., Zagloel, T.Y.M., Harwahyu, R., Asvial, M., Suryanegara, M., Kusrini, E., Kartohardjono, S., Sahlan, M., Putra, N., Budiyanto, M.A., 2022. Accelerating innovation in the industrial revolution 4.0 era for a sustainable future. *International Journal of Technology*, Volume 13(5), pp. 944-948

Tong, J., Xue, M., Zhu, Z., Wang, W., Tian, S., 2022. Impacts of morphological characteristics on target strength of chub mackerel (*Scomber japonicus*) in the Northwest Pacific Ocean. *Frontiers in Marine Science,* Volume ~~54(6), pp. 1006-1022~~9, p. 856483

~~Urick, R.J., 1983. *Principles of Underwater Sound. 3rd Edition*. McGraw-Hill, New York~~

Triyanto, T., Haryani, G.S., Lukman, L., Wibowo, H., Ali, F., Hidayat, H., Sulawesty, F., Setiawan, F.A., Triwisesa, E., Dwinovantyo, A., Riyanto, M., Samir, O., Nafisyah, E., 2021. Perspective plan for sustainable eel management in Lake Poso, Central Sulawesi. *E3S Web of Conferences,* Volume 322, p. 05014

Winfield, I.J., Fletcher, J.M., James, J.B., Bean, C.W., 2009. Assessment of fish populations in still waters using hydroacoustics and survey gill netting: Experiences with Arctic charr (*Salvelinus alpinus*) in the UK. *Fisheries Research,* Volume 96-(1), pp. 30-38

Zang, X., Yin, T., Hou, Z., Mueller, R.P., Deng, Z.D., Jacobson, P.T., 2021. Deep learning for automated detection and identification of migrating American eel *Anguilla rostrata* from imaging sonar data. *Remote Sensing*, Volume 13(14), p. 2671